



Deposited via The University of York.

White Rose Research Online URL for this paper:

<https://eprints.whiterose.ac.uk/id/eprint/130198/>

Version: Accepted Version

Article:

Becerra-Rivera, Victor A., Bergström, Ed, Thomas-Oates, Jane et al. (2018) Polyamines are required for normal growth in sinorhizobium meliloti. Microbiology (Reading, England). 000615. pp. 600-613. ISSN: 1465-2080

<https://doi.org/10.1099/mic.0.000615>

Reuse

Items deposited in White Rose Research Online are protected by copyright, with all rights reserved unless indicated otherwise. They may be downloaded and/or printed for private study, or other acts as permitted by national copyright laws. The publisher or other rights holders may allow further reproduction and re-use of the full text version. This is indicated by the licence information on the White Rose Research Online record for the item.

Takedown

If you consider content in White Rose Research Online to be in breach of UK law, please notify us by emailing eprints@whiterose.ac.uk including the URL of the record and the reason for the withdrawal request.

1 Polyamines are required for normal growth in *Sinorhizobium meliloti*

2

3

4 Victor A. Becerra-Rivera¹, Ed Bergström², Jane Thomas-Oates² and Michael F.
5 Dunn^{1*}

6

7

8 **Author affiliations:** ¹Programa de Genómica Funcional de Procariotes, Centro de
9 Ciencias Genómicas, Universidad Nacional Autónoma de México, Cuernavaca,
10 Morelos 62210, Mexico. ²Centre of Excellence in Mass Spectrometry and
11 Department of Chemistry, University of York, Heslington, York, YO10 5DD, UK.

12 ***Correspondence:** Michael F. Dunn, mike@ccg.unam.mx

13 **Key words:** *S. meliloti*; polyamines; putrescine; spermidine; homospermidine;
14 norspermidine; ornithine decarboxylase

15 **Abbreviations:** ADC, arginine decarboxylase; Agm, agmatine; Arg, L-arginine; L-
16 Asp β-SA, L-aspartate β-semialdehyde; Cad, cadaverine; Cb, carbenicillin; CID,
17 collision induced dissociation; DAP, 1,3-diaminopropane; DNS, dansyl group;
18 DNSCl, dansyl chloride; DNS-PA, dansyl-polyamine; FT-ICR, Fourier-transform ion
19 cyclotron resonance; Gm, gentamicin; Gus, β-glucuronidase; *gusA*, gene encoding
20 β-glucuronidase; HPTLC, high performance thin layer chromatography; HSpd,
21 homospermidine; Km, kanamycin; LB, Luria-Bertani; Lys, L-lysine; LDC, lysine
22 decarboxylase; MALDI, matrix-assisted laser desorption/ionisation; MMS, minimal
23 medium succinate-ammonium; MMS-acid, MMS medium, pH 5.5; MMS-Salt, MMS
24 medium with 0.3 M NaCl; MS, mass spectrometry; MS/MS, tandem mass
25 spectrometry; μ, generations h⁻¹; Nm neomycin; NSpd, norspermidine; OD₆₀₀,
26 optical density at 600 nm; ODC, ornithine decarboxylase; *odc1*, gene encoding
27 ornithine decarboxylase SMa0680; *odc2*, gene encoding lysine/ornithine
28 decarboxylase SMc02983; Orn, L-ornithine; PA, polyamine; Put, putrescine; PY,
29 peptone-yeast extract; Sp, spectinomycin; Spd, spermidine; Spm, spermine; Sm,
30 streptomycin; TCA, trichloroacetic acid; TSS, transcriptional start site.

31 One supplementary table and one supplementary figure are available with the
32 online Supplementary Material.

33 **Subject category:** Physiology and metabolism

34 **Word count:** 6,279

35

36 **Abstract**

37 Polyamines (PAs) are ubiquitous polycations derived from basic L-amino acids
38 whose physiological roles are still being defined. Their biosynthesis and functions
39 in nitrogen-fixing rhizobia such as *Sinorhizobium meliloti* have not been extensively
40 investigated. Thin layer chromatographic and mass spectrometric analyses
41 showed that *S. meliloti* Rm8530 produces the PAs putrescine (Put), spermidine
42 (Spd) and homospermidine (HSpd) in their free forms and norspermidine (NSpd) in
43 a form bound to macromolecules. The *S. meliloti* genome encodes two putative
44 ornithine decarboxylases (ODC) for Put synthesis. Activity assays with the purified
45 enzymes showed that ODC2 (SMc02983) decarboxylates both ornithine and
46 lysine. ODC1 (SMa0680) decarboxylates only ornithine. An *odc1* mutant was
47 similar to the wild type in ODC activity, PA production and growth. In comparison
48 to the wild type, an *odc2* mutant had 45 % as much ODC activity and its growth
49 rates were reduced by 42, 14 and 44 % under non-stress, salt stress or acid stress
50 conditions, respectively. The *odc2* mutant produced only trace levels of Put, Spd
51 and HSpd. Wild type phenotypes were restored when the mutant was grown in
52 cultures supplemented with 1 mM Put or Spd or when the *odc2* gene was
53 introduced *in trans*. *odc2* gene expression was increased under acid stress and
54 reduced under salt stress and with exogenous Put or Spd. An *odc1 odc2* double
55 mutant had phenotypes similar to the *odc2* mutant. These results indicate that
56 ODC2 is the major enzyme for Put synthesis in *S. meliloti* and that PAs are
57 required for normal growth *in vitro*.

58

59 **INTRODUCTION**

60 Polyamines (PAs) are low molecular weight organic compounds with two or more
61 amino groups that are positively charged at neutral pH [1]. With few exceptions,
62 PAs are ubiquitous in all organisms and have important roles in processes as
63 diverse as growth, stress resistance and the regulation of transcription and
64 translation in both eukaryotes and prokaryotes [2-5]. In contrast to their essential
65 functions in eukaryotes and archaea, the physiological roles of PAs in bacteria are
66 less clearly defined. In prokaryotes, PAs are involved in biofilm formation, stress

67 resistance, motility, pathogenesis, and growth. [6-12]. This diversity of functions
68 might explain the presence of the more varied PA repertoire in bacteria [5].

69

70 Diamines found in bacteria include putrescine (Put), cadaverine (Cad) and 1,3-
71 diaminopropane (DAP) (Fig. 1). Put is produced by nearly all bacteria, Cad is
72 common in Proteobacteria and DAP is found sporadically in diverse phyla.
73 Spermidine (Spd) is the most commonly found triamine, though bacteria may
74 produce the related homospermidine (HSpd) and/or, less commonly,
75 norspermidine (NSpd) [2,5,13].

76

77 Put can be made by the decarboxylation of L-ornithine (Orn) by Orn decarboxylase
78 (ODC; EC 4.1.1.17) or of L-arginine (Arg) by Arg decarboxylase (ADC; EC
79 4.1.1.19). The ADC reaction produces agmatine (Agm), which is converted to Put
80 by agmatinase (SpeB; EC 3.5.3.11). Cad is produced by lysine decarboxylase
81 (LDC; EC 4.1.1.18) acting on L-lysine (Lys). Some decarboxylases have activity
82 with both Lys and Orn as substrates [5,13,14].

83

84 In *Sinorhizobium meliloti* and other nitrogen-fixing rhizobia, work on PAs has
85 focused on their identification and quantification during free-living growth [15,16],
86 changes in their levels *in nodulo* when host plants were subjected to abiotic stress,
87 or determining the effects of exogenous polyamines on symbiosis [12,17-21]. A
88 few studies using biochemical and genetic approaches have shown species-
89 dependent requirements for different PAs for growth, biofilm formation and motility
90 in rhizobia [11,22-25].

91

92 Three studies with different strains of *S. meliloti* grown in minimal medium show
93 that its free PA fraction invariably contains Put, Spd and HSpd, with Cad found in
94 two of the studies [15,16,19]. Hamana et al. [16] assayed for, but did not detect,
95 Agm, spermine (Spm), NSpd or DAP in *S. meliloti* IAM 12611. PAs in *S. meliloti*
96 1021 have been reported only for cultures grown in rich medium, where Put, Spd,
97 HSpd and Spm were detected [19]; the latter probably originates from Spm present

98 in the tryptone and yeast extract components of the medium [14]. In contrast to
99 other rhizobia, the genome sequence of strain 1021 indicates that it is able to
100 synthesize NSpd, which has not been reported in rhizobia, and possesses an
101 "alternative" pathway for Spd synthesis [14]. The strain 1021 genome encodes
102 three putative basic amino acid decarboxylases. *sma0682* is annotated as a
103 "decarboxylase (lysine, ornithine, arginine)" but its genomic context and sequence
104 suggest that it encodes an ADC. We predicted that *sma0680* (annotated as "amino
105 acid (ornithine, lysine, arginine) decarboxylase") encodes an ODC: we denominate
106 this gene and enzyme as *odc1* and ODC1, respectively. *smc02983* is annotated as
107 an "ornithine, DAP, or arginine decarboxylase" but its product has sequence
108 characteristics that suggest it is able to decarboxylate both lysine and ornithine
109 [14,26]. We refer here to the *smc02983* gene and protein product as *odc2* and
110 ODC2, respectively (Fig. 1).

111

112 Because *S. meliloti* has multiple enzymes catalyzing the conversion of *N*-
113 acetylornithine to Orn during Arg biosynthesis [27] and is also able to produce Orn
114 with an inducible arginase [14,26], we hypothesized that Orn is the major precursor
115 for Put synthesis in this organism [27]. If this is correct, then ODC1 and/or ODC2
116 should be the key enzyme(s) for the synthesis of Put and the PAs derived from it
117 (Fig. 1). The work presented here shows that ODC2 is responsible for synthesizing
118 the majority of the Put produced by *S. meliloti* and that PAs are important for
119 normal growth in minimal medium cultures with and without abiotic stress.

120

121 **METHODS**

122 **Bacterial strains, plasmids and culture growth conditions**

123 Bacterial strains and plasmids are listed in Table 1. PY and LB complex media,
124 and MMS minimal medium with succinate and NH₄Cl as carbon and nitrogen
125 sources, respectively, were described previously [27]. Salt stress was caused by
126 growing cultures in MMS-salt medium, where NaCl was added to MMS to a final
127 concentration of 0.3 M before adjusting the pH to 6.8 and autoclaving. For growth
128 under acidic stress, MMS-acid medium was prepared by adjusting MMS medium to

129 pH 5.5 (rather than 6.8) before autoclaving. PA and amino acid supplements were
130 prepared as 0.5 M stocks, adjusted to pH 6.8 (for use in MMS and MMS-salt) or pH
131 5.5 (for use in MMS-acid) and filter sterilized. To grow *S. meliloti* strains, cells from
132 3 day PY plates with appropriate antibiotics were used to inoculate 3 ml of liquid
133 PY containing the same antibiotics and incubated at 200 rpm, 30°C. After 24 h, 1
134 ml of these cultures were used to inoculate 50 ml of PY containing one-half the
135 normal concentration of antibiotics, in 125 ml baffled flasks. These cultures were
136 incubated as above for 24 h, harvested by centrifugation at 5500 x g for 5 min, the
137 cells washed twice in MMS and resuspended to an OD₆₀₀ of approximately 1.5 in
138 MMS. These suspensions were used to inoculate the desired minimal medium
139 without antibiotics to an initial OD₆₀₀ of 0.05: for transcriptional fusion and PA
140 analyses, respectively, the medium:baffled flask volume ratios were 50:125 ml and
141 100:250 ml. Cultures were grown with agitation at 200 rpm at 30°C and growth
142 was monitored at 600 nm. Specific growth rates (μ , generations h⁻¹) were
143 calculated [28] from culture OD₆₀₀ values obtained between 4 and 12 h under non-
144 stress conditions and 4 to 24 h under stress conditions. When required, antibiotics
145 were used at the following concentrations ($\mu\text{g ml}^{-1}$): carbenicillin (Cb), 50;
146 gentamicin (Gm), 15; kanamycin (Km), 50; neomycin (Nm), 60; spectinomycin
147 (Sp), 100; streptomycin (Sm), 200.

148

149 **DNA manipulations**

150 Standard protocols were used to grow *E. coli* and for DNA isolation, restriction
151 digests, cloning and transformation [29]. Bacterial conjugations were performed as
152 described previously [27]. High-stringency DNA hybridizations were done with a
153 DIG-High Prime DNA Labeling kit (Roche).

154

155

156 **PCR amplifications**

157 DNA sequences were obtained from GenBank (www.ncbi.nlm.nih.gov/gene/).
158 Primers (Table S1, Supplementary material) were used in PCR reactions with
159 Accuprime Taq DNA polymerase (Invitrogen) to clone genes for the construction of
160 transcriptional fusions or whose products were to be overexpressed and purified,
161 or with Dream Taq PCR master mix (Thermo) for other purposes. PCR cycling
162 programs included a denaturing step at 95°C for 1 min followed by 30 cycles of
163 95°C for 1 min, 56°C for 1 min and 72°C for a time appropriate for the length of the
164 DNA being amplified. A final elongation step was made at 72°C for 10 min. For
165 use in cloning, PCR products were purified with a commercially available kit.

166

167 **Recombinant protein purification**

168 *S. meliloti* genes *odc1* and *odc2* were amplified by PCR (Table S1) and cloned in
169 pET Sumo to generate plasmids pSumo-*odc1* and pSumo-*odc2* (Table 1). These
170 plasmids were used to overexpress the corresponding 6His-Sumo tagged protein
171 products in *E. coli* BL21(DE3). For overexpression and purification, strain
172 BL21(DE3) transformed with either pSumo-*odc1* or pSumo-*odc2* were grown in
173 100 ml LB Km at 37°C, 200 rpm to an OD₆₀₀ of 0.4, IPTG was added to a final
174 concentration of 1 mM and incubation continued for 8 and 14 h, respectively. 6His-
175 Sumo tagged proteins were purified using Ni-NTA resin (Invitrogen) under hybrid
176 conditions following the manufacturer's protocol.

177

178 **Mutant construction**

179 Mutants of *S. meliloti* Rm8530 were constructed by the insertional inactivation of
180 genes as described previously [27]. Briefly, genome regions encoding *odc1* and
181 *odc2* were amplified by PCR (Table S1) and cloned into pCR 2.1-Topo to produce
182 plasmids pCRodc1 and pCRodc2 (Table 1). Following verification by restriction
183 enzyme analysis, the inserts from pCRodc1 and pCRodc2 were excised with
184 *SmaI/XbaI* and *SaII*, respectively, and inserted into suicide vector pK18mobsacB
185 cut with *SmaI/XbaI* or *XhoI* to give plasmids pKodc1 and pKodc2 respectively. The
186 loxP Sp cassette from pMS102loxSp17 was ligated into the *Bam*HI and *SaII* sites

187 of the genes cloned in pKodc1 and pKodc2, respectively, generating plasmids
188 pKodc1::loxSp and pKodc2::loxSp (Table 1). These constructs were introduced
189 into *S. meliloti* Rm8530 by triparental mating using *E. coli* DH5 α /pRK2013 as
190 helper. A Sp^r Nm^r single recombinant obtained from each mating was spread on
191 PY containing Sm, Sp and 12 % sucrose to allow the selection of the 8530 *odc1*
192 and 8530 *odc2* mutants (Table 1). The 8530 *odc1 odc2* double mutant was
193 constructed in two steps. First, the loxP Sp interposon in the *odc1* gene in the 8530
194 *odc1* mutant was deleted by introducing plasmid pBBRMCre, which expresses the
195 loxP-specific Cre recombinase, into the mutant. The desired loxP Sp deletion and
196 pBBRMCre plasmid-cured strain was selected by screening for the Sm^r Sp^s and
197 Sm^r Gm^s phenotypes, respectively [30]. In the second step, plasmid pKodc2::loxSp
198 was introduced into the 8530 *odc1* loxSp-deleted mutant to obtain the 8530 *odc1*
199 *odc2* double mutant by selection for sucrose sensitivity. The correct construction of
200 the mutants was confirmed by Southern hybridization.

201

202 **Genetic complementation of the 8530 *odc2* mutant**

203 To test genetic complementation of the *odc2* mutant, we excised the *EcoRI*
204 fragment from pCRodc2, which contains the *odc2* gene with its native promoter
205 and terminator regions, and introduced it into pBB5 to give plasmid pBB5-*odc2*.
206 This plasmid, or pBB5 without an insert, was introduced into the 8530 *odc2* mutant
207 by triparental mating.

208

209 **Basic amino acid decarboxylase assays**

210 The radiochemical assay for determining ODC activity in intact cells was modified
211 from that of Romano et al. [31]. Cells from 16 h cultures were washed twice with
212 100 mM potassium phosphate buffer, pH 7 (KP 7) and resuspended to an OD₆₀₀ of
213 3.0. Assay mixtures (250 μ l) contained 100 mM KP 7, 4.5 mM MgSO₄, 3 mM β -
214 mercaptoethanol and 85 nM pyridoxal-5'-phosphate. Individual reactions were
215 started by adding L-ornithine to a final concentration of 3.5 mM containing 0.025
216 μ Ci of L-[1-¹⁴C]-ornithine. Assay mixtures were deposited in plastic tubes in which
217 a CO₂ trap consisting of a 2 x 2.5 cm piece of filter paper wet with 125 μ l of 1 M

218 NaOH was placed so as to adhere to the top portion of the tube. Fifty μ l aliquots of
219 cell suspension were added to the tubes, which were sealed with rubber septa and
220 incubated for 4 h at 30°C. Reactions were stopped by adding 200 μ l of 10 %
221 trichloroacetic acid (TCA) and samples were re-capped and left at room
222 temperature for one hour. The paper CO₂ traps were mixed with 10 ml of Ultima
223 Gold LSC cocktail (Sigma) and radioactivity determined by liquid scintillation
224 counting. One unit (U) of activity is defined as the production of 1 nmol CO₂ min⁻¹
225 mg protein⁻¹. Total cellular protein was determined as described previously [32].
226 Decarboxylase activities of the purified 6His-Sumo-ODC1 or 6His-Sumo-ODC2
227 enzymes were determined using colorimetric assays with Arg [33], Orn [34] or Lys
228 [35] as substrates. Assay of purified enzymes was done using 25-30 μ g of purified
229 6His-Sumo-ODC1 or 6His-Sumo-ODC2 per reaction and 1 U of activity is defined
230 as the production of 1 nmol of decarboxylation product min⁻¹ mg protein⁻¹. Protein
231 concentrations were determined by the Bradford method [36].

232

233 **Construction of a *odc2* transcriptional fusion with the β -glucuronidase** 234 **(*gusA*) gene**

235 *odc2* is the first gene of a predicted two gene operon but does not contain a
236 predicted transcription start site (TSS) [37]. The PCR primers used to amplify the
237 upstream and 5' coding region of *odc2* are described in Table S1, and the
238 amplified region was cloned into pTZ57R/T (Table 1). The *gusA* fusion with this
239 gene, plasmid pBB53odc2::*gusA*, was constructed using the PCR product of *odc2*
240 that includes the 586 nt intergenic region between its start codon and that of the
241 divergently transcribed *smc02984* gene, 19 and 297 nt of the of the *smc02984* and
242 *odc2* coding regions, respectively. A clone containing the pTZ57R/T plasmid with
243 the PCR product in the desired orientation was identified by digestion with
244 appropriate restriction enzymes. The insert from the plasmid was excised with
245 *Apal/XbaI* and cloned into vector pBBMCS-53 cut likewise, transcriptionally fusing
246 the *odc2* promoter/5' region to the *gusA* gene. The correct transcriptional
247 orientation of the fusion plasmid was confirmed by restriction enzyme digestion and
248 in PCR reactions with primer p53lw (reverse primer specific for *gusA*) and the

249 forward primer for *odc2* (Table S1; [27]). The fusion plasmid was transferred to *S.*
250 *meliloti* Rm8530 by triparental mating.

251

252 **β -glucuronidase (Gus) assays**

253 Experimental cultures were grown in the desired minimal medium for 16 h at 30°C
254 with shaking at 200 rpm. Gus activity was determined by measuring the production
255 of *p*-nitrophenol from the *p*-nitrophenyl β -D-glucuronide substrate with quantitation
256 based on total protein [27]. One unit (U) of activity is defined as the production of 1
257 nmol of product $\text{min}^{-1} \text{mg protein}^{-1}$. Strain Rm8530 containing pBBMCS-53 without
258 an insert lacked Gus activity under the growth conditions tested.

259

260 **Polyamine analysis by High Performance Thin-Layer Chromatography** 261 **(HPTLC)**

262 Dansyl (DNS) derivatives of PAs were analyzed by HPTLC using modifications of
263 previously published protocols [38,39]. Cells from 32 h cultures were pelleted by
264 centrifugation at 5500 x *g* for 5 min and resuspended to an OD₆₀₀ of 3.0 in fresh
265 MMS. Cells from 1 ml portions of these suspensions were pelleted at 13,200 x *g*,
266 resuspended with 0.5 ml of 5 % (w/v) TCA and stored at 4°C for 18-24 h. Free
267 PAs present in the TCA supernatants, obtained by centrifugation at 13,200 x *g* for
268 10 min, were derivatized in 2 ml glass vials by mixing 40 μl of the supernatant, 80
269 μl of dansyl-chloride (DNSCI) solution (5 mg ml^{-1} in acetone) and 40 μl of
270 supersaturated aqueous sodium carbonate. Reaction mixtures containing PA
271 standards (1.2 μg of the PA in 40 μl of 5 % TCA) were derivatized in the same way.
272 The capped vials were heated at 80°C for 1 h, cooled to room temperature and
273 quenched with 20 μl of L-proline solution (150 mg ml^{-1} in water) for 30 min at room
274 temperature in darkness. The reaction mixtures were extracted twice with 100 μl of
275 toluene and the combined extracts dried under a stream of N₂. Samples of DNS-
276 PA standards and DNS-PAs from cells were resuspended with 100 and 45 μl of
277 toluene, respectively. One μl of DNS-PA standards or 10 μl of DNS-PAs from cells
278 were run on Silica Gel 60 HPTLC plates (Merck) using chloroform/triethylamine
279 (5:1 v/v) as mobile phase. For the routine determination of PAs produced by *S.*

280 *meliloti* cells from cultures, only the free PA fraction was analyzed. PAs can exist
281 as free molecules in the cytoplasm or as forms bound to macromolecules such as
282 proteins, lipids or nucleic acids. These bound forms of PAs can be obtained in
283 their free forms by strong acid hydrolysis of the TCA-precipitated macromolecules
284 [14]. We analyzed PAs bound to macromolecules as follows. Pellets of insoluble
285 material obtained from treating cells with 5 % TCA were washed with 0.5 ml of 5 %
286 TCA and the pellets resuspended with 0.5 ml of 6 N HCl. The suspensions were
287 heated at 110°C for 18-24 h in 2 ml V-Vials with teflon-lined caps (Sigma). Twenty
288 µl of hydrolysate was combined with 40 µl each of the DNSCI and supersaturated
289 sodium carbonate solutions described above, and derivatization and HPTLC
290 carried out as for free PAs. Plates were visualized under UV light and images
291 captured with a Syngene (Frederick, MD, USA) InGenius imaging system.
292 Densitometric quantification was done using ImageJ 1.48v software. For mass
293 spectrometric analysis, the silica gel corresponding to DNS-PA spots were scraped
294 off the TLC plates and eluted with methanol. After passage through 0.22 µM
295 cellulose acetate filter units (Costar), methanol was removed under a N₂ stream.
296 The samples were reconstituted in 200 µl acetonitrile:H₂O (1:1; v:v) containing
297 0.25% (v:v) formic acid.

298

299 **Mass spectrometric analysis of dansyl-PAs**

300 MALDI mass spectra were acquired using a Bruker 9.4T solariX XR Fourier-
301 transform ion cyclotron resonance (FT-ICR) mass spectrometer (Bremen,
302 Germany). The samples were ionized in positive ion mode using the MALDI ion
303 source with α-cyano-4-hydroxycinnamic acid (CHCA) matrix. Sample spots were
304 produced by premixing 1.4 µl of sample solution with the same volume of matrix
305 solution (saturated solution in acetonitrile:H₂O (1:1; v:v) containing 0.25% (v:v)
306 formic acid); 1 µl of this mixture was spotted onto a stainless steel target plate and
307 allowed to air dry at ambient temperature. Spectra were measured with a transient
308 length of 2.2 s resulting in a resolving power of 400000 at *m/z* 400. The instrument
309 was externally calibrated using a standard peptide mix and a 'lock-mass' calibration
310 was used with the matrix ion with *m/z* 568.135. Collision induced dissociation

311 (CID) was used to generate product ions and was achieved in the hexapole
312 collision cell using argon as the collision gas. Product ion spectra were recorded
313 with a transient length of 1.1 s, giving a resolution of 200000 at m/z 400.

314

315 **RESULTS AND DISCUSSION**

316 **Identification of PAs produced by *S. meliloti* Rm8530**

317 The work reported here uses *S. meliloti* Rm8530 as wild type. This strain is
318 identical to the sequenced and well-characterized strain 1021 except that it has a
319 functional copy of the *expR* gene, whose product is involved in quorum-sensing
320 based transcriptional regulation [40]. PA production by strain Rm8530 has not
321 been reported previously. By HPTLC analysis, we found no quantitative or
322 qualitative differences in the PAs produced by strains 1021 and Rm8530 grown
323 under the conditions reported here (results not shown).

324

325 Selected *S. meliloti* dansyl-PA (DNS-PA) derivatives and DNS-derivatives of
326 authentic PA standards were isolated from HPTLC plates (Fig. S1 (a),
327 Supplementary material) and analyzed by MALDI high resolution, high mass
328 accuracy FT-ICR mass spectrometry (MS) and product ion tandem mass
329 spectrometry (MS/MS). The details of this analysis are described in Fig. S1,
330 Supplementary material. The reason for this analysis was to unambiguously identify
331 DNS-PA spots present on our HPTLC plates, and this was particularly important for
332 HSpd, for which no commercial standard is available, and for NSpd, which has not
333 been reported in rhizobia.

334

335 As mentioned, PA analyses of various *S. meliloti* grown in culture showed the
336 presence of Put, Spd, HSpd and (usually) Cad, but not Agm, spermine (Spm),
337 NSpd or DAP. Our analysis of the PAs produced by strain Rm8530 grown in MMS
338 (Fig. S1) shows the presence of Put, Spd, HSpd and NSpd, with the latter found
339 only in the bound PA fraction. The presence of NSpd only in the bound fraction
340 explains why it has not been detected previously in *S. meliloti*. Our results also
341 indicate that Cad (or a Cad-like compound) is produced. We tentatively identified

342 DAP in cells from PA-supplemented cultures (described later), while neither Agm
343 nor Spm were detected under any growth condition (results not shown).

344

345 **Amino acids decarboxylated by ODC1 and ODC2**

346 To provide a biochemical basis for our assignment of the ODC1 and ODC2
347 proteins as a monofunctional ODC and a bifunctional Lys/ODC, respectively, we
348 purified each as 6His-Sumo-tagged proteins and tested their ability to
349 decarboxylate Arg, Lys and Orn. Neither protein had detectible activity with Arg as
350 substrate. With Orn, the 6His-Sumo-ODC1 had a specific activity of 4.1 U, but no
351 activity with Lys as substrate. The 6His-Sumo-ODC2 had specific activities of 8.6
352 and 0.9 U using Orn and Lys, respectively, as substrates. These results match our
353 prediction of the substrates decarboxylated by each enzyme [14].

354

355 **ODC2 is the major enzyme for Put synthesis in *S. meliloti***

356 To determine the importance of ODC1 and ODC2 in PA synthesis, we constructed
357 single and double mutants of strain Rm8530 in which the encoding gene(s) were
358 inactivated (Table 1). Because both the *odc1* and *odc2* genes are present in
359 operons [37], the inactivation of either gene probably also prevents the
360 transcription of downstream gene(s) in the operons. For *odc1*, the downstream
361 genes encode a Put transporter (PotE; SMa0678) and a ABC transporter substrate
362 binding protein possibly for glutamate/aspartate (SMa0677). The products of these
363 genes are probably not the only ones responsible for Put or glutamate/aspartate
364 transport, since *S. meliloti* encodes an additional Put ABC transporter and three
365 Spd/Put ABC transporters, in addition to numerous amino acid transport systems,
366 both general and specific [14,26]. The single downstream gene (*smc02982*) in
367 operon with *odc2* encodes a possible *N*-acetyltransferase that we proposed might
368 function in the production of *N*-acetylglutamate for Orn and Arg biosynthesis [26,
369 41]. We found, however, that a *smc02982* null mutant of *S. meliloti* 1021 was an
370 Arg prototroph that grew normally on MMS [41].

371

372 Cultures of the wild type and mutants were grown in MMS and their ability to
373 decarboxylate Orn was determined. In comparison to the wild type, the ODC
374 activities of the Rm8530 *odc1*, *odc2* and *odc1 odc2* mutants were decreased by
375 14, 55 and 75 %, respectively (Fig. 2). We conclude that it is much more likely that
376 these reductions in ODC activity result from the inactivation of *odc1* and/or *odc2*
377 rather than of downstream genes in their operons. From these results we estimate
378 that all but about 25 % of the total ODC activity in strain Rm8530 is due to the
379 combined activities of the ODC1 and ODC2, with the latter enzyme accounting for
380 about 80 % of this. The remaining ODC activity in the double mutant could result
381 from the predicted ADC (SMa0682) being able to decarboxylate Orn in addition to
382 or instead of Arg, or by the conversion of the ¹⁴C-Orn assay substrate to ¹⁴C-Arg by
383 enzymes of the Arg biosynthesis pathway [27], with subsequent decarboxylation of
384 the ¹⁴C-Arg by the ADC.

385

386 The wild type and mutant strains were grown in MMS under control (non-stress) or
387 abiotic stress conditions to determine how inactivating the decarboxylases affected
388 growth and PA production (Fig. 3). Estimations of relative changes in PA levels
389 were made by densitometry of DNS-PA spots on HPTLC plates from at least two
390 independent experiments. Specific growth rates (generations h⁻¹) for selected
391 cultures are shown in Fig. 4. The growth of the mutant strains in PY rich medium
392 was indistinguishable from that of the wild type (results not shown).

393

394 In wild type Rm8530 grown under control conditions, HSpd, Spd and Put account
395 for virtually all of the DNS-PAs detected by HPTLC (Fig. 3(d)): relative to this total
396 quantity set at 1.0, the proportions comprised by each of the three polyamines are
397 0.31, 0.56 and 0.13, respectively. During growth under the control, saline or acidic
398 conditions, the *odc1* mutant grew similarly to the wild type (Fig. 3 (a) - (c)) and its
399 content of HSpd, Spd and Put differed from the wild type by less than 10 %. In
400 contrast, the *odc2* single and *odc1 odc2* double mutants grew about 40 % slower
401 than the wild type or the *odc1* mutant (Fig. 4) and reached a lower cell yield under
402 all conditions, most notably with acid stress (Fig. 3(a)-(c)). In the rhizobial plant

403 pathogen *Agrobacterium tumefaciens* strain C58, an *odc* deletion mutant produced
404 much less Put and Spd and grew more slowly than the wild type in minimal
405 medium [25]. The *A. tumefaciens* ODC and the *S. meliloti* ODC2 share over 90 %
406 deduced amino acid sequence identity and may thus fulfill similar physiological
407 functions.

408

409 In the wild type under saline stress (Fig. 3(d)), HSpd was undetectable and Put
410 decreased by > 90 %, but Spd levels were maintained at a high level similar to that
411 seen under control conditions. HSpd levels decrease in salt-stressed
412 *Sinorhizobium fredii* P220 (a relatively salt- and acid-resistant strain), where it was
413 proposed that having less of this polycation offsets the increase in positive charges
414 caused by the rise in cytosolic K⁺ that occurs under these conditions [18]. With
415 acidic stress, wild type Rm8530 had a nearly 4-fold decrease in Put, while HSpd
416 and Spd levels remained constant. In *S. fredii* P220 HSpd levels increase 2-fold
417 at pH 4 as compared to pH 9.5, which is an acidic stress much more drastic than
418 the pH 5.5 versus pH 6.8 stress that we imposed on *S. meliloti* in our experiments.
419 Under acidic conditions, HSpd may provide cytosolic buffering or protect
420 macromolecules from acid denaturation [18].

421

422 PA levels in the *odc1* mutant differed by no more than 10 % from the wild type
423 under all of the growth conditions tested. The *odc2* mutant grown under control
424 conditions lacked detectable Put and produced 9 and 18 % the wild type levels of
425 HSpd and Spd, respectively. It also contained some apparent NSpd in the free
426 fraction that accounted for 4.3 % of the total PAs. The PA profile of the *odc1 odc2*
427 double mutant from control cultures was similar to that of the *odc2* single mutant
428 (including the presence of free NSpd), except that Put was present at 11 % of the
429 wild type level. The reduction in growth caused by the inactivation of the *S. meliloti*
430 *odc2* is similar to what occurs in *R. leguminosarum* and *A. tumefaciens* when Put
431 synthesis is lowered by treatment with the ODC inhibitor dimethylfluoroornithine or
432 by inactivation of the *odc* gene, respectively [23,25]. In both the *odc2* and double

433 mutants, the levels of Put, Spd and HSpd were also markedly lower than in the wild
434 type during growth under salt or acid stress (Fig. 3 (d)).

435 **Chemical complementation restores growth and PA levels in the *odc2* mutant**

436 Testing the ability of an exogenous PA to restore the normal phenotype of a PA
437 mutant is called chemical complementation [9,11,23,24]. The effect of chemical
438 complementation on the specific growth rate (μ , or generations h^{-1} ; Fig. 4) and PA
439 content (Fig. 5) of the Rm8530 wild type and selected PA mutants was determined
440 under control, salt stress and acid stress conditions. For these experiments, we
441 used exogenous Put and Spd for chemical complementation since these PAs
442 result directly or indirectly from Orn decarboxylation (Fig. 1). HSpd is derived
443 directly from Put but was not tested because it is not commercially available. NSpd
444 was used for chemical complementation since its synthesis does not require Put
445 (Fig. 1).

446

447 In control (non-stressed) cultures without added PAs, μ values of the *odc1*, *odc2*
448 and *odc1 odc2* mutants were 93, 59 and 60 % that of the wild type (Fig. 4(a)). The
449 specific growth rate of the *odc1* mutant grown under stress or non-stress
450 conditions with or without exogenous PAs differed from the wild type by no more
451 than 13 %, in contrast to the much more pronounced growth defects found in the
452 *odc2* and *odc1 odc2* mutants. As mentioned, the levels of Put, HSpd and Spd in
453 the *odc1* mutant are comparable to those of the wild type, while they are similarly
454 and drastically reduced to low levels in the *odc2* and double mutants (Fig. 3(d)). In
455 cultures without added PAs, growth under salt and acidic stress reduced the μ of
456 Rm8530 by 21 and 27 %, respectively, in comparison to non-stress conditions (Fig.
457 4). Under salt stress conditions, the μ values of the mutants were less affected
458 relative to the wild type grown under the same condition, with the *odc1*, *odc2* and
459 double mutants having 102, 86 and 85 % wild type growth rates (Fig. 4(b)). This
460 may occur because *S. meliloti* responds to salt stress by lowering its total PA
461 content (Fig. 3(d)), and so the *odc2* and double mutants, with their very low PA
462 levels, are less affected for growth under saline conditions than under control
463 conditions. Under acid stress, the *odc1*, *odc2* and double mutants had μ values of

464 105, 57 and 55 % of wild type (Fig. 4(c)). Thus, under this stress condition, the
465 lack of ODC1 activity has essentially no effect on growth, while the mutants lacking
466 ODC2 activity have growth reductions similar to that found under control
467 conditions.

468

469 For wild type Rm8530 grown under control (non-stress) conditions (Fig. 4(a)),
470 exogenous Put or Spd caused a reduction in μ of 8-9 % and NSpd caused a 21 %
471 decrease. Lesser decreases in wild type μ values were caused by the PAs under
472 salt stress (reductions of 4, 6 and 12 % for Put, Spd and NSpd, respectively).
473 Under acid stress, wild type μ values decreased 7 % with Put, increased 1.1 fold
474 with Spd and were unchanged with NSpd. For the *odc2* and double mutant grown
475 under stress or non-stress conditions, Put supplementation restored μ to 94 to 96
476 % that of wild type. When these mutants were grown under control or salt stress
477 conditions, exogenous Spd restored growth rates to 89-96 % that of wild type,
478 while under acid stress it allowed growth at slightly higher than wild type μ values
479 (Fig. 4). When grown in NSpd-supplemented cultures under non-stress conditions,
480 the growth of the *odc2* and double mutants were restored to only 66 and 69 % that
481 of wild type, respectively. Under salt and acid stress, these values ranged from 79-
482 89 % of wild type. Thus, exogenous NSpd was not as effective as Put or Spd in
483 restoring the growth of *odc2* and double mutants under any growth condition. It is
484 interesting to note that the growth restoration caused with NSpd was greater under
485 stress than non-stress conditions.

486

487 Under control conditions, Rm8530 cells from cultures grown with 1 mM Put (Fig.
488 5(a)) had 77 % less Put, 30 % less Spd and 1.9-fold more HSpd relative to cells
489 grown without added Put (Fig. 3(d) and results not shown). Cells from the Put-
490 supplemented cultures also contained a trace of DAP, which accounted for than 1
491 % of the total PAs present (Fig. 5(a)). The decrease in Put might result from its
492 use in HSpd synthesis. DAP is not derived from Put and it is not known whether
493 Put can modulate the production of PAs in the L-aspartate β -semialdehyde (L-Asp
494 β -SA) branch of the synthesis pathway (Fig. 1).

495 Supplementation of Rm8530 control cultures with Spd caused a modest (13 %)
496 decrease in intracellular Spd concentration, a 1.6-fold increase in Put and no
497 change in HSpd, but caused the appearance of detectable DAP (Fig. 3(d) and Fig.
498 5(b) and results not shown). As described later, the drastic reduction in *odc2*
499 transcription observed in cells from Spd-supplemented cultures suggests that the
500 nearly unchanged level of intracellular Spd could result from its reduced synthesis
501 by ODC2 being offset by the uptake of exogenous Spd. Whether the increase in
502 Put is derived from the retroconversion of Spd to Put, as occurs in *A. tumefaciens*
503 [11], is unknown. In Spd-supplemented MMS-salt cultures, HSpd was
504 undetectable while Put and DAP levels were greatly decreased in comparison to
505 their levels in the control cultures. Under these conditions, Spd was the only PA
506 present at high levels. Cultures grown under acidic conditions with added Spd
507 produced significantly less HSpd and Put than non-stressed cultures, but had the
508 same or slightly higher levels of DAP. For all of the strains grown under all
509 conditions, the addition of NSpd to the medium resulted in a high level of its
510 accumulation, an apparent total absence of Spd and at most trace levels of HSpd
511 and Put, and remarkably high amounts of DAP (Fig. 5(c)). In *A. tumefaciens*, cells
512 grown in the presence of NSpd (which is not produced by this organism) also
513 produce little intracellular Spd [25]. In *S. meliloti*, the intriguing possibility exists
514 that NSpd has regulatory effects on the production on PAs derived from Put.

515

516 **Genetic complementation restores growth and PA levels in the *odc2* mutant**

517 To confirm that the inactivation of the *odc2* gene was responsible for the altered
518 phenotype of the *odc2* mutant, we introduced the *odc2* gene into the mutant on
519 plasmid pBB5-*odc2* (Table 1). The resulting transconjugant, 8530 *odc2*(pBB5-
520 *odc2*), had its Orn decarboxylating activity restored to nearly that of the wild type,
521 while the activity in the mutant containing the cloning vector alone (strain 8530
522 *odc2*(pBB5)) was very similar to that of the uncomplemented mutant (Fig. 2).
523 Strain 8530 *odc2*(pBB5-*odc2*) also grew similarly to the wild type under stress and
524 non-stress growth conditions, and its ability to produce PAs was restored to
525 approximately wild type levels (Fig. 6). These results are consistent with the

526 inactivation of the *odc2* gene being the cause of the growth and PA production
527 phenotypes of the *odc2* mutant. The *odc2* mutant also produced some apparent
528 NSpd in the free PA fraction (Fig. 6(d)). In comparison to the uncomplemented
529 mutant, strain 8530 *odc2*(pBB5) had a slower growth rate under all conditions,
530 perhaps due to the metabolic burden of plasmid maintenance. As expected, strain
531 8530 *odc2*(pBB5) produced low levels of PAs similar to the mutant without the
532 plasmid (Fig. 6).

533

534 Although the introduction of genes for metabolic enzymes cloned on plasmid pBB5
535 into *S. meliloti* can increase the gene products activity several-fold, presumably
536 due to increased copy number [27], we did not find increased in ODC activity (Fig.
537 2) or over-production of PAs (Fig 6(d)) in strain 8530 *odc2*(pBB5-*odc2*).

538

539 **Transcriptional expression of *odc2* under different growth conditions**

540 The expression of β -glucuronidase (*gusA*) transcriptional fusions to the *odc1* and
541 *odc2* genes was determined in strain Rm8530 grown under different growth
542 conditions. The *odc1* gene is part of a predicted four gene operon and lacks a
543 transcriptional start site (TSS) [37]: we found that a *odc1::gusA* fusion produced a
544 low level of Gus activity (50-115 nmol min⁻¹ mg protein⁻¹). *In vivo*, *odc1*
545 transcription may be linked to that of the upstream gene (*smc0682*), which is not
546 part of the fusion construct.

547

548 Under the growth conditions tested, the GUS specific activity from the *odc2::gusA*
549 fusion changed over a 7-fold range, from about 400 to 2900 nmol min⁻¹ mg protein⁻¹
550 (Fig. 7). Although *odc2* also lacks a recognizable TSS, it is the first gene in an
551 apparent two-gene operon [37] and the results described below suggest that *odc2*
552 expression is modulated in response to growth conditions.

553

554 In comparison to control (non-stress) conditions, *odc2* transcription decreased 69
555 % under salt stress (Fig. 7), consistent with the 94 % reduction in Put in these cells
556 (Fig 3(d) and results not shown). The decreased Put content in salt stressed cells

557 is not explained by its conversion to HSpd and/or Spd, since the combined quantity
558 of these PAs was nearly identical in the control and salt-stressed cells. Decreased
559 expression of *odc2* was also reported in a transcriptomic study of *S. meliloti* 1021
560 grown under salt stress [42]. Acidic stress increased *odc2* transcription 1.5-fold,
561 which does not correlate with the 77 % decrease in Put levels seen during growth
562 at low pH (Fig. 3(d)).

563

564 Cells grown in cultures supplemented with the exogenous Put precursor amino
565 acids Arg or Orn expressed *odc2* at a level 20 and 28 % less than in cells from
566 unsupplemented cultures. Assigning these effects solely to the exogenous amino
567 acid added to the cultures is complicated by the ability of *S. meliloti* to convert Arg
568 to Orn using arginase and to metabolize Orn to Arg by activities of the Arg
569 synthesis pathway [14]). We can tentatively conclude that Orn, the major substrate
570 for ODC2, does not induce *odc2* expression.

571

572 To determine the effect of exogenous PAs on *odc2* transcription, we used Put and
573 Spd, which result directly and indirectly from Orn decarboxylation, respectively, and
574 DAP and NSpd, which are not derived from Put (Fig 1). Exogenous Put, Spd and
575 NSpd inhibited *odc2* transcription by 58, 79 and 36 % respectively, while DAP
576 resulted in a small increase in its transcription (Fig. 7). Thus, the PA products
577 resulting from Orn decarboxylation inhibited *odc2* transcription to a greater degree
578 than the PAs from the L-Asp β -SA branch of the pathway.

579

580 In summary, we have shown that Put and/or PAs derived from it are required for
581 the normal growth of *S. meliloti* Rm8530. ODC2 (SMc02983) is a bifunctional
582 Lys/Orn decarboxylase responsible for synthesizing the majority of Put produced
583 by strain Rm8530, and changes in *odc2* transcription observed under some growth
584 conditions are consistent with observed changes in PA levels. The *S. meliloti*
585 ODC1 (SMa0680) is a monofunctional ODC that contributes a minor portion of the
586 ODC activity in Rm8530.

587

588 The results presented here provide a basis for further experiments aimed at
589 deciphering the enzymology and regulation of PA metabolism in *S. meliloti*, which
590 provides an attractive model system due to its extended PA biosynthetic
591 capabilities [14]. We are currently addressing some of these questions, along with
592 determining the physiological roles of specific PAs in free-living and symbiotically-
593 associated *S. meliloti*.

594

595 **Funding information**

596 Work at the UNAM was supported by DGAPA-PAPIIT Grants IN210114 and
597 IN206317 to M. F. D. The York Centre of Excellence in Mass Spectrometry was
598 created thanks to a major capital investment through Science City York, supported
599 by Yorkshire Forward with funds from the Northern Way Initiative, and subsequent
600 support from EPSRC (EP/K039660/1; EP/M028127/1).

601

602 **Acknowledgements**

603 Victor A. Becerra-Rivera is a doctoral student from Programa de Doctorado en
604 Ciencias Biomédicas, Universidad Nacional Autónoma de México (UNAM) and
605 received fellowship 574042 from CONACYT. We thank María J. Soto
606 (Departamento de Microbiología del Suelo y Sistemas Simbióticos de la Estación
607 Experimental del Zaidín, CSIC, Granada, Spain) for providing *S. meliloti* strain
608 Rm8530 and Lourdes Girard (CCG-UNAM) for providing the p53lw primer and the
609 pBBRMCre plasmid.

610

611 **Conflict of interest**

612 The authors declare that there are no conflicts of interest.

613

614 **References**

- 615 1. Tabor CW, Tabor H. Polyamines. *Annu Rev Biochem* 1984;53:749-790.
- 616 2. Hamana K, Matsuzaki S. Polyamines as a chemotaxonomic marker in bacterial
617 systematics. *Crit Rev Microbiol* 1992;18:261-283.

- 618 3. Algranati ID. Polyamine metabolism in *Trypanosoma cruzi*: studies on the
619 expression and regulation of heterologous genes involved in polyamine
620 biosynthesis. *Amino Acids* 2010;38:645-51.
- 621 4. Miller-Fleming L, Olin-Sandoval V, Campbell K, Ralser M. Remaining mysteries
622 of molecular biology: The role of polyamines in the cell. *J Mol Biol*
623 2015;427:3389–3406.
- 624 5. Michael AJ. Polyamines in eukaryotes, bacteria, and archaea. *J Biol Chem*
625 2016;291:14896-14903.
- 626 6. Soksawatmaekhin W, Kuraishi A, Sakata K, Kashiwagi K, Igarashi K, Excretion
627 and uptake of cadaverine by CadB and its physiological functions in
628 *Escherichia coli*. *Mol Microbiol* 2004;51:1401–1412.
- 629 7. Sturgill G, Rather PN. Evidence that putrescine acts as an extracellular signal
630 required for swarming in *Proteus mirabilis*. *Mol Microbiol* 2004;51:437-446.
- 631 8. Shah P, Swiatlo E. A multifaceted role for polyamines in bacterial pathogens.
632 *Mol Microbiol* 2008;68:4–16.
- 633 9. Lee J, Sperandio V, Frantz DE, Longgood J, Camilli A *et al*. An alternative
634 polyamine biosynthetic pathway is widespread in bacteria and essential for
635 biofilm formation in *Vibrio cholerae*. *J Biol Chem* 2009;284:9899-907.
- 636 10. Cockerell SR, Rutkovsky AC, Zayner JP, Cooper RE, Porter LR *et al*. *Vibrio*
637 *cholerae* NspS, a homologue of ABC-type periplasmic solute binding
638 proteins, facilitates transduction of polyamine signals independent of their
639 transport. *Microbiology* 2014;160:832-843.
- 640 11. Kim SH, Wang Y, Khomutov M, Khomutov A, Fuqua C, Michael AJ. The
641 essential role of spermidine in growth of *Agrobacterium tumefaciens* is
642 determined by the 1,3-diaminopropane moiety. *ACS Chem Biol*
643 2016;11:491-9.
- 644 12. López-Gómez M, Hidalgo-Castellanos J, Lluch C, Herrera-Cervera JA.
645 Epibrassinolide ameliorates salt stress effects in the symbiosis *Medicago*
646 *truncatula*-*Sinorhizobium meliloti* and regulates the nodulation in cross-talk
647 with polyamines. *Plant Physiol Biochem* 2016;108:212-221.

- 648 13. Lucas PM. Ornithine and lysine decarboxylation in bacteria. In: D'Mello FJ
649 (editor) *Handbook of Microbial Metabolism of Amino Acids*. Wallingford,
650 Oxfordshire: CAB International; 2017. pp. 116-127.
- 651 14. Dunn MF. Rhizobial Amino Acid Metabolism: Polyamine Biosynthesis and
652 Functions. In: D'Mello FJ (editor) *Handbook of Microbial Metabolism of*
653 *Amino Acids*. Wallingford, Oxfordshire: CAB International; 2017. pp. 352-
654 370.
- 655 15. Hamana K, Minamisawa K, Matsuzaki S. Polyamines in *Rhizobium*,
656 *Bradyrhizobium*, *Azorhizobium* and *Agrobacterium*. *FEMS Microbiol Lett*
657 1990;71: 71-76.
- 658 16. Hamana K, Sakamoto A, Tachiyanagi S, Terauchi E, Takeuchi M. Polyamine
659 profiles of some members of the alpha subclass of the class Proteobacteria:
660 Polyamine analysis of twenty recently described genera. *Microbiol Cult Coll*
661 2003;19:13-21.
- 662 17. Vassileva V, Ignatov, G. Polyamine-induced changes in symbiotic parameters
663 of the *Galega orientalis-Rhizobium galegae* nitrogen-fixing system. *Plant*
664 *Soil* 1999;210:83-91.
- 665 18. Fujihara S, Yoneyama T. Effects of pH and osmotic stress on cellular
666 polyamine contents in the soybean rhizobia *Rhizobium fredii* P220 and
667 *Bradyrhizobium japonicum* A1017. *Appl Environ Microbiol* 1993;59:1104-
668 1109.
- 669 19. López-Gómez M, Hidalgo-Castellanos J, Iribarne C, Lluch C. Proline
670 accumulation has prevalence over polyamines in nodules of *Medicago*
671 *sativa* in symbiosis with *Sinorhizobium meliloti* during the initial response to
672 salinity. *Plant Soil* 2014;374: 149-159.
- 673 20. Palma F, López-Gómez M Tejera NA, Lluch C. Involvement of abscisic acid in
674 the response of *Medicago sativa* plants in symbiosis with *Sinorhizobium*
675 *meliloti* to salinity. *Plant Sci* 2014;223:16-24.
- 676 21. López-Gómez M, Hidalgo-Castellanos J, Muñoz-Sánchez JR, Marín-Peña AJ,
677 Lluch C, Herrera-Cerver, JA. Polyamines contribute to salinity tolerance in

- 678 the symbiosis *Medicago truncatula*-*Sinorhizobium meliloti* by preventing
679 oxidative damage. *Plant Physiol Biochem* 2017;116:9-17.
- 680 22. Braeken K, Daniels R, Vos K, Fauvart M, Debkumari Bachaspatimayum D,
681 Vanderleyden J, Michiels J. Genetic determinants of swarming in *Rhizobium*
682 *etli*. *Microbial Ecol* 2008;55:54-64.
- 683 23. Shaw FL. *From prediction to function: Polyamine biosynthesis and formate*
684 *metabolism in the α - and ϵ -Proteobacteria*. Ph.D Thesis. England: Institute
685 of Food Research, Norwich Research Park; 2011.
- 686 24. López-Gómez M, Cobos-Porras L, Prell J, Lluch C. Homospermidine synthase
687 contributes to salt tolerance in free-living *Rhizobium tropici* and in symbiosis
688 with *Phaseolus vulgaris*. *Plant Soil* 2016;404:413–425.
- 689 25. Wang Y, Kim SH, Natarajan R, Heindl JE, Brugerm EL *et al*. Spermidine
690 inversely influences surface interactions and planktonic growth in
691 *Agrobacterium tumefaciens*. *J Bacteriol* 2016;198:2682-2691.
- 692 26. Dunn MF. Key roles of microsymbiont amino acid metabolism in rhizobia-
693 legume interactions. *Crit Rev Microbiol* 2015;41:411-451.
- 694 27. Hernández VM, Girard L, Hernández-Lucas I, Vázquez A, Ortiz-Ortiz C *et al*.
695 Genetic and biochemical characterization of arginine biosynthesis in
696 *Sinorhizobium meliloti* 1021. *Microbiology* 2015;161:1671-1682.
- 697 28. Dunn MF, Araíza G, Cevallos MA, Mora J. Regulation of pyruvate carboxylase
698 in *Rhizobium etli*. *FEMS Microbiol Lett* 1997;157:301-306.
- 699 29. Sambrook J, Fritsch EF, Maniatis T. *Molecular Cloning: A Laboratory Manual*
700 New York: Cold Spring Harbor Laboratory Press; 1989.
- 701 30. Landeta C, Dávalos A, Cevallos MA, Geiger O, Brom S, Romero D. Plasmids
702 with a chromosome-like role in Rhizobia. *J Bacteriol* 2011;193:1317-1326.
- 703 31. Romano A, Trip H, Lolkema JS, Lucas PM. Three-component lysine/ornithine
704 decarboxylation system in *Lactobacillus saerimneri* 30a. *J Bacteriol*
705 2013;195:1248-1254.
- 706 32. Girard L, Brom S, Dávalos A, López O, Soberón M, Romero, D. Differential
707 regulation of *fixN*-reiterated genes in *Rhizobium etli* by a novel *fixL*-*fixK*
708 cascade. *Mol Plant-Microbe Interact* 2000;13:1283-1292.

- 709 33. Goldschmidt MC, Lockhart BM. Rapid methods for determining decarboxylase
710 activity: arginine decarboxylase. *Appl Microbiol* 1971;22:350-357.
- 711 34. Ngo TT, Brillhart KL, Davis RH, Wong RC, Bovaird JH *et al.*
712 Spectrophotometric assay for ornithine decarboxylase. *Anal Biochem*
713 1987;160:290-293.
- 714 35. Phan APH, Ngo TT, Lenhoff HM. Spectrophotometric assay for lysine
715 decarboxylase. *Anal Biochem* 1982;120:193-197.
- 716 36. Bradford MM. A rapid and sensitive method for the quantitation of microgram
717 quantities of protein utilizing the principle of protein-dye binding. *Anal*
718 *Biochem* 1976;72:248-254.
- 719 37. Schlüter JP, Reinkensmeier J, Barnett MJ, Lang C, Krol E, Giegerich R, *et al.*
720 Global mapping of transcription start sites and promoter motifs in the
721 symbiotic α -proteobacterium *Sinorhizobium meliloti* 1021. *BMC Genomics*
722 2013;14:156.
- 723 38. Slocum RD, Flores HE, Galston AW, Weinstein LH. Improved method for
724 HPLC analysis of polyamines, agmatine and aromatic monoamines in plant
725 tissue. *Plant Physiol* 1989;89:512-517.
- 726 39. Pedrol N, Tiburcio AF. Polyamines determination by TLC and HPLC. In: Roger
727 MJR (editor). *Handbook of Plant Ecophysiology Techniques*. The
728 Netherlands: Kluwer Academic Publishers; 2001. pp. 335–363.
- 729 40. Pellock BJ, Teplitski M, Boinay RP, Bauer WD, Walker GC. A LuxR homolog
730 controls production of symbiotically active extracellular polysaccharide II by
731 *Sinorhizobium meliloti*. *J Bacteriol* 2002;184:5067-5076.
- 732 41. Paulino, EM. Búsqueda del gen que codifica para la enzima *N*-acetilglutamato
733 sintasa por mutagénesis. Bachelors Thesis. Mexico: Universidad Autónoma
734 del Estado de Morelos; 2013.
- 735 42. Domínguez-Ferreras A, Pérez-Arnedo R, Becker A, Olivares J, Soto MJ,
736 Sanjuán J. Transcriptome profiling reveals the importance of plasmid
737 pSymB for osmoadaptation of *Sinorhizobium meliloti*. *J Bacteriol*
738 2006;188:7617-7625.

- 739 43. Kovach ME, Elzer PH, Hill DS, Robertson GT, Farris MA *et al.* Four new
740 derivatives of the broad-host-range cloning vector pBBR1MCS, carrying
741 different antibiotic-resistance cassettes. *Gene* 1995;160:175-176.
- 742 44. Schäfer A, Tauch A, Jäger W, Kalinowski J, Thierbach G, Pühler A. Small
743 mobilizable multi-purpose cloning vectors derived from the *Escherichia coli*
744 plasmids pK18 and pK19: selection of defined deletions in the chromosome
745 of *Corynebacterium glutamicum*. *Gene* 1994;145:69-73.
- 746 45. Martínez-Salazar JM, Romero D. Role of *ruvB* gene in homologous
747 recombination in *Rhizobium etli*. *Gene* 2000;243:125-131.
- 748 46. Figurski DH, Helinski DR. Replication of an origin-containing derivative of
749 plasmid RK2 dependent on a plasmid function provided in trans. *Proc Natl*
750 *Acad Sci (USA)* 1979;76:1648-1652.

751

752

753

754

755

756

757

758 **Table 1.** Strains and plasmids used in this study.

759

Strain or plasmid	Relevant characteristics	Source or reference
<i>E. coli</i> strains		
BL21(DE3)	Strain for protein expression	Invitrogen
DH5 α	Cloning strain	Laboratory collection
JM109	Cloning strain	Laboratory collection
<i>S. meliloti</i> strains		
Rm8530	<i>S. meliloti</i> 1021 <i>expR</i> ⁺ , Sm ^r	M. Soto, Estación Experimental del Zaidín, CSIC, Granada, Spain
8530 <i>odc1</i>	Rm8530 <i>sma0680::loxP</i> Sp <i>odc1</i> null mutant, Sm ^r Sp ^r	This study
8530 <i>odc2</i>	Rm8530 <i>smc02983::loxP</i> Sp <i>odc2</i> null mutant, Sm ^r Sp ^r	This study
8530 <i>odc1 odc2</i>	Rm8530 <i>sma0680::loxP smc02983::loxP</i> Sp <i>odc1 odc2</i> null double mutant, Sm ^r Sp ^r	This study
8530 <i>odc2</i> (pBB5)	Rm8530 <i>smc02983::loxP</i> Sp <i>odc2</i> null mutant containing plasmid pBB5, Sm ^r Sp ^r Gm ^r	This study
8530 <i>odc2</i> (pBB5- <i>odc2</i>)	Rm8530 <i>smc02983::loxP</i> Sp <i>odc2</i> null mutant complemented with the <i>odc2</i> gene <i>in trans</i> , Sm ^r Sp ^r Gm ^r	This study
Plasmids		
pBB5	Broad-host-range vector pBBR1MCS-5, Gm ^r	[43]
pBB5- <i>odc2</i>	pBBR1MCS-5 containing <i>smc02983</i> with native promoter and terminator regions, Gm ^r	This study
pBBMCS-53	Δ <i>placZ</i> pBBR1MCS-5 derivative	[32]

	with promoterless <i>gusA</i> , Gm ^r	
pBB53odc1:: <i>gusA</i>	Transcriptional <i>sma0680</i> :: <i>gusA</i> fusion in pBBMCS-53	This study
pBB53odc2:: <i>gusA</i>	Transcriptional <i>smc02983</i> :: <i>gusA</i> fusion in pBBMCS-53	This study
pCRodc1	Rm8530 genome region containing <i>odc1</i> cloned in pTopo	This study
pCRodc2	Rm8530 genome region containing <i>odc2</i> cloned in pTopo	This study
pKodc1	Rm8530 genome region containing <i>odc1</i> cloned in pK18mobsacB	This study
pKodc2	Rm8530 genome region containing <i>odc2</i> cloned in pK18mobsacB	This study
pK18mobsacB	Broad-host range gene replacement vector, Km ^r	[44]
pKodc1:: <i>loxSp</i>	<i>odc1</i> :: <i>loxP</i> Sp fragment cloned in pK18mobsacB	This study
pKodc2:: <i>loxSp</i>	<i>odc2</i> :: <i>loxP</i> Sp fragment cloned in pK18mobsacB	This study
pMS102 <i>loxSp</i> 17	Source of the <i>loxP</i> Sp interposon, Sp ^r	[45]
pRK2013	Helper plasmid, Km ^r	[46]
pET-Sumo	Expression vector for production of 6His-Sumo-tagged proteins, Km ^r	Invitrogen
pSumo-odc1	pET-Sumo containing the cloned Rm8530 <i>odc1</i> gene	This study
pSumo-odc2	pET-Sumo containing the cloned Rm8530 <i>odc2</i> gene	This study
pTopo	pCR2.1Topo vector for cloning PCR products, Km ^r	Invitrogen
pTZ57R/T	InstAclone vector for cloning PCR	Thermo

products, Ap^r (Cb^r)

pBBRMCre

Plasmid used for deleting the loxP [30]

Sp interposon inserted in *smc0680*

760

761

762

763

764 **FIGURE LEGENDS**

765

766 **Fig. 1.** Predicted polyamine synthesis pathways in *S. meliloti* Rm8530.
767 Abbreviations not described in the text: α -KG, α -ketoglutarate; CNSpd,
768 carboxynorspermidine; CANSDC, CNSpd decarboxylase; CANSDH, CNSpd
769 dehydrogenase; CSpd; carboxyspermidine; DABA, diaminobutyric acid; DABA AT,
770 DABA aminotransferase; DABA DC, DABA decarboxylase; L-Glu, L-glutamate;
771 HSS, homospermidine synthase. Modified from [14].

772

773 **Fig. 2.** Specific activities of Orn decarboxylation by *S. meliloti* strains grown in
774 MMS, normalized to that of the Rm8530 wild type (100 % = 3968 U). Values are
775 the mean \pm SD for two independent experiments. Values for columns marked with
776 the same letter are not statistically different according to a t-student test.

777

778 **Fig. 3.** Growth and PA content of *S. meliloti* cultured under non-stress and stress
779 conditions. Panels (a), (b) and (c) represent culture growth under control, salt
780 stress and acidic stress conditions, respectively. Strains and line colors: Rm8530
781 wild type, black; 8530 *odc1*, pink; 8530 *odc2*, green; 8530 *odc1 odc2*, blue. Panel
782 (d) shows HPTLC detection of dansyl-PAs from 32 h cultures. Lane S contains
783 dansyl-PA standards with their identities shown at the right side of the first plate
784 image. *S. meliloti* dansyl-PA samples are: Lane 1, Rm8530; Lane 2, 8530 *odc1*;
785 Lane 3, 8530 *odc2*; Lane 4, 8530 *odc1 odc2*.

786

787 **Fig 4.** Specific growth rates (μ , generations h^{-1}) of selected *S. meliloti* strains
788 grown in MMS with or without chemical complementation with exogenous PAs.
789 Panel (a), control conditions; panel (b), MMS-salt; panel (c), MMS-acid. The PA
790 added to the cultures is indicated at the bottom of the figure. Bar colors represent:
791 Rm8530 wild type, blue; 8530 *odc1*, orange; 8530 *odc2*, grey; 8530 *odc1 odc2*,
792 yellow. Values are normalized to μ values of the wild type grown under the three
793 conditions in media lacking added PAs, where 100 % corresponds to μ values of

794 0.179, 0.141 and 0.130 for the MMS, MMS-salt and MMS-acid cultures. Results
795 are the mean \pm SD for 2 independent experiments.

796

797 **Fig. 5.** Effect of chemical complementation with exogenous PAs on PA production
798 by *S. meliloti* strains. HPTLC detection of dansyl-PAs from 32 h cultures. Lane S
799 contains dansyl-PA standards with their identities shown at the left side of the
800 plates. Panel (a), MMS plus 1 mM Put; panel (b), MMS plus 1 mM Spd; panel (c),
801 MMS plus 1 mM NSpd. Lane assignments for all plates: Lane 1, Rm8530 wild type;
802 Lane 2, 8530 *odc1*; Lane 3, 8530 *odc2*; Lane 4, 8530 *odc1 odc2*.

803

804 **Fig. 6.** Growth and PA content of the genetically complemented 8530 *odc2* mutant.
805 Panels (a), (b) and (c) show culture growth under control, salt stress and acidic
806 stress conditions, respectively. Strains and line colors: Rm8530 wild type, black;
807 8530 *odc2*, green; 8530 *odc2*(pBB5-*odc2*), red; 8530 *odc2*(pBB5), purple. Panel
808 (d) shows HPTLC detection of dansyl-PAs from 32 h cultures. Lane S contains
809 dansyl-PA standards with their identities shown at the left side of the plate. *S.*
810 *meliloti* dansyl-PA samples are: Lane 1, Rm8530; Lane 2, 8530 *odc2*; Lane 3,
811 8530 *odc2*(pBB5); Lane 4, 8530 *odc2*(pBB5-*odc2*).

812

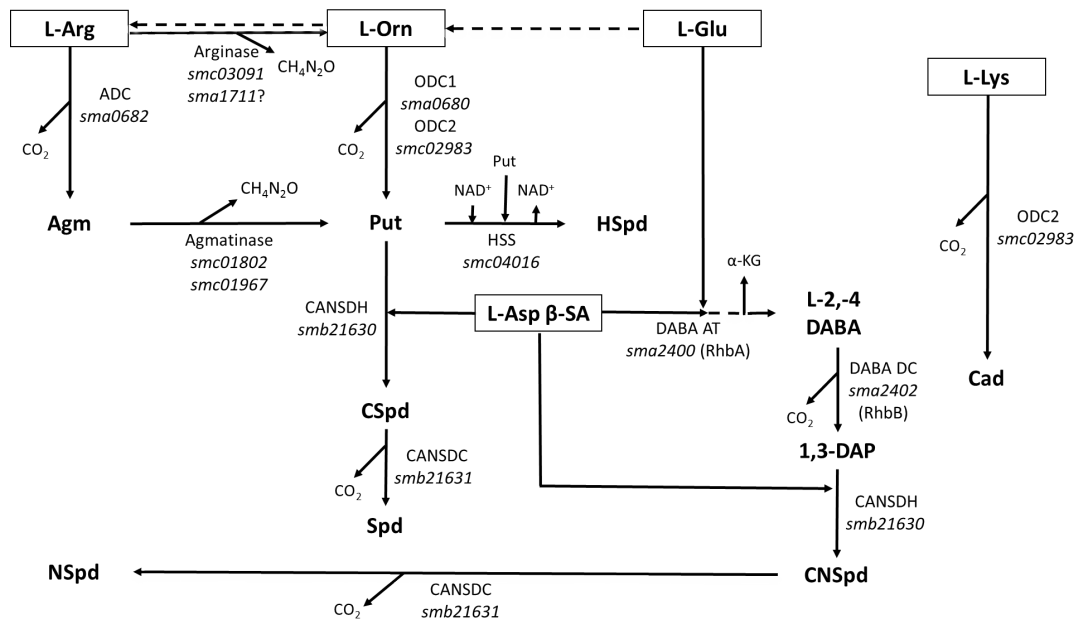
813 **Fig. 7.** β -glucuronidase (Gus) activities produced by *S. meliloti* Rm8530 containing
814 the *odc2::gusA* transcriptional fusion plasmid. Cells were grown in the indicated
815 media for 16 h. Values are the mean \pm SD for two independent experiments, each
816 with 2 technical replicates of two biological replicates. 1 U = nmol product min⁻¹ mg
817 protein⁻¹.

818

819

820

821

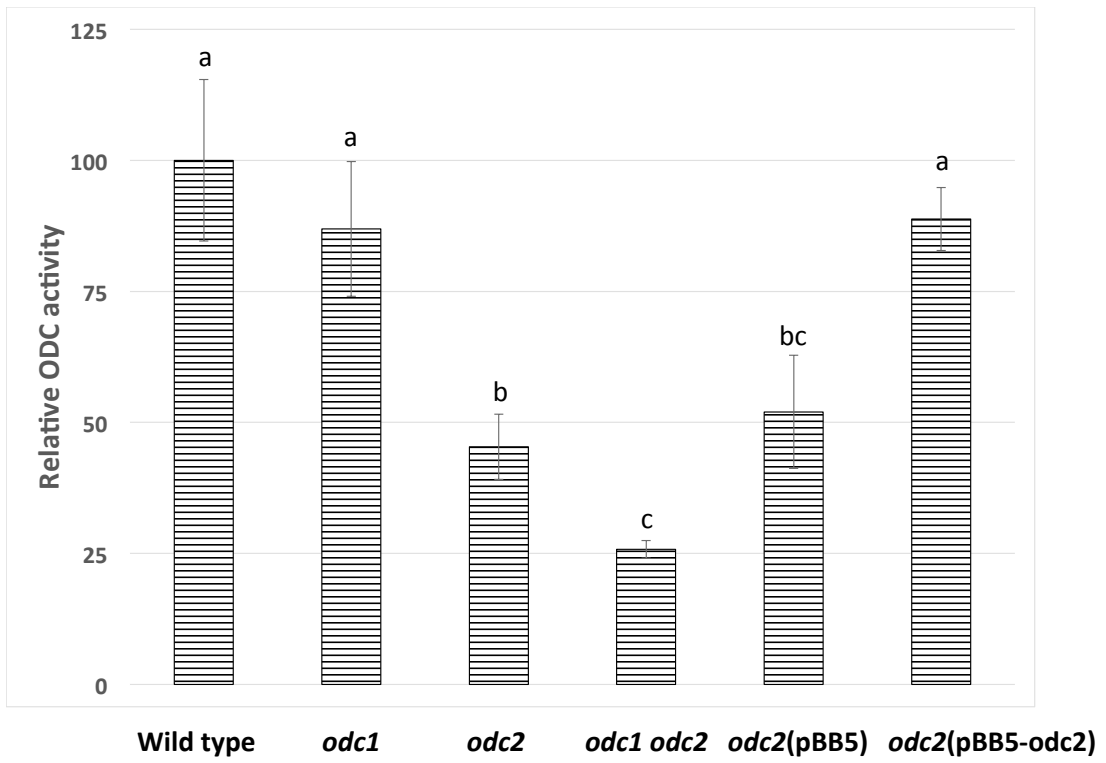


822

823 Fig. 1

824

825

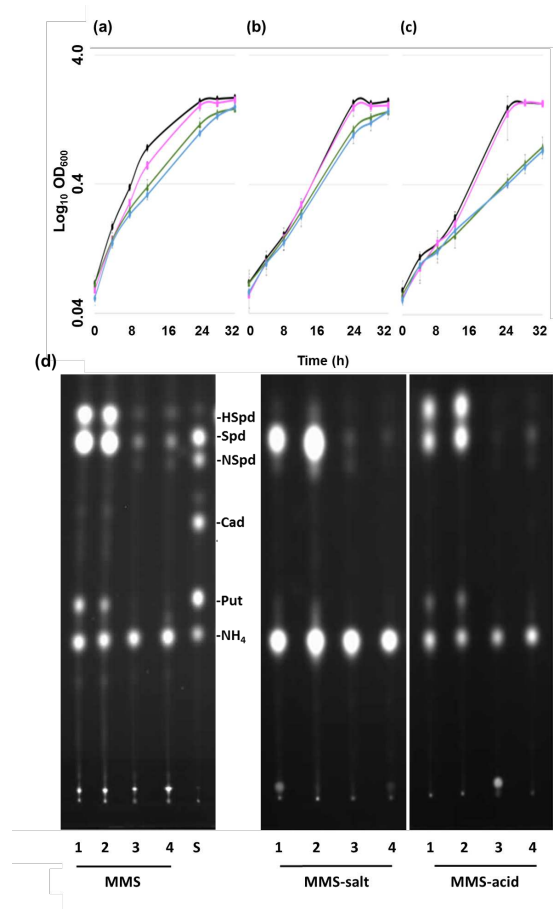


826

827

828 Fig. 2

829



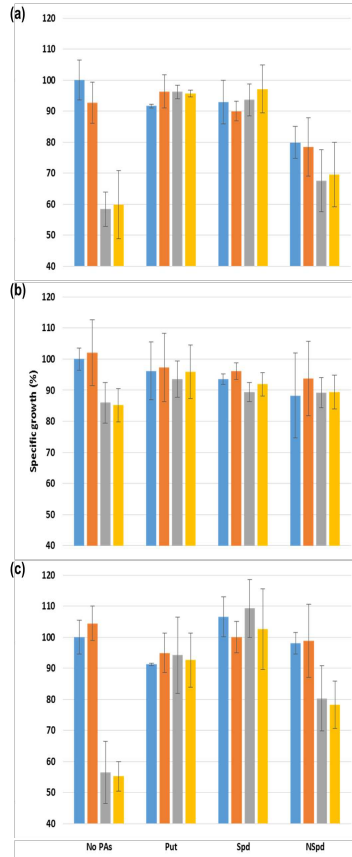
830

831

832

833

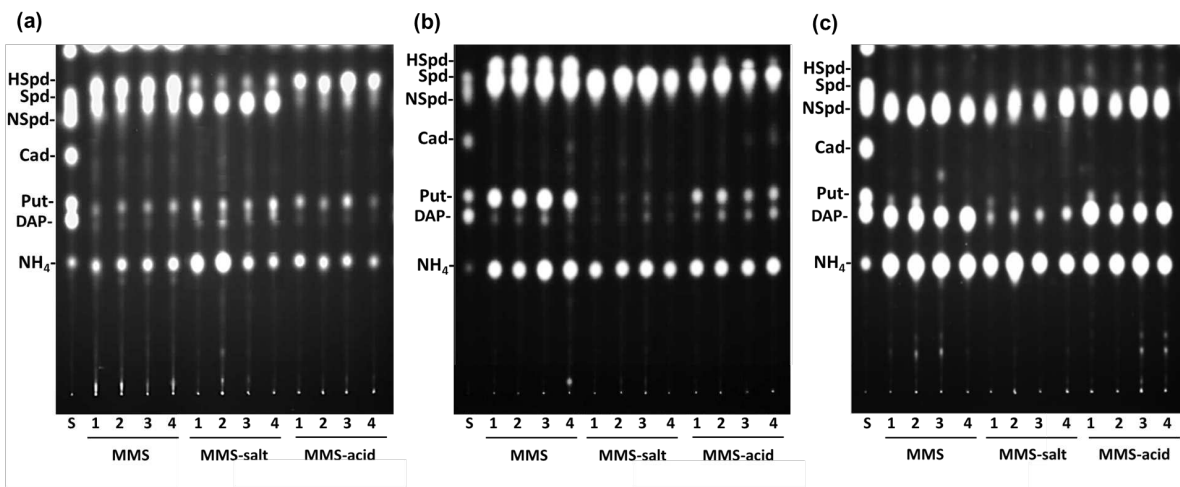
834 Fig. 3



835
836 Fig. 4

837

838



839

840

841

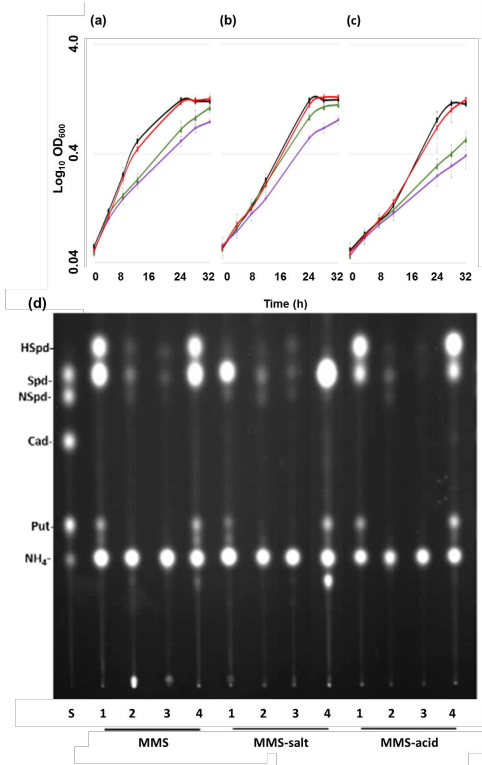
842

843

844

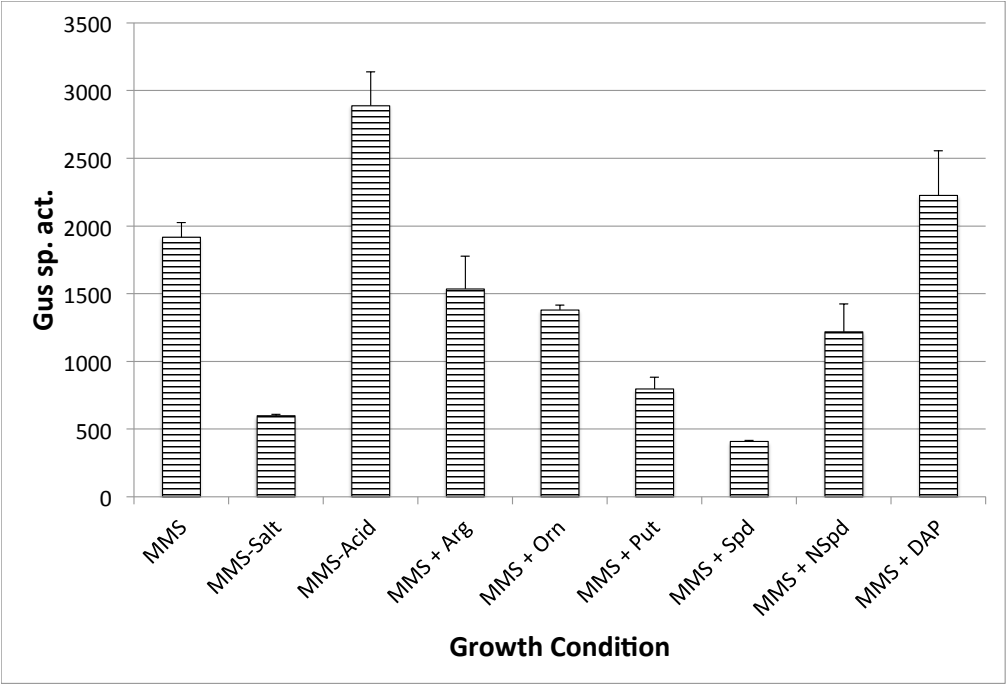
845 Fig. 5

846



847 Fig. 6
848

849



850

851

852 Fig. 7

853

854 **Supplementary material**855 **Table S1.** Oligonucleotide primers used in this study.

Primer name	5'-3' nucleotide sequence	Description
Sumo0680F	GTGAAGGCTCCGACCGTC	Forward primer for amplifying the insert used in making pSumo-odc1 and pCR-odc1
Sumo0680R	GATTACTCGCGCACGGCG	Reverse primer for amplifying the insert used in making pSumo-odc1 and pCR-odc1
Sumo02983F	ATGGCCATGACCACCGC	Forward primer for amplifying the insert used in making pSumo-odc2
Sumo02983R	GGATCAGATGACATAGGCC	Reverse primer for amplifying the insert used in making pSumo-odc2
F-02983	TTG GCA CGC ACG AGATCG	Forward primer for amplifying the insert used in making pCR-odc2
R-02983	GGATCAGATGACATAGGCC	Reverse primer for amplifying the insert used in making pCR-odc2
0680gusF	CTACAACCGCCTGGTCAAG	Forward primer used in construction of pBB53odc1::gusA
0680gusR	TCCCAATATAGGCACCAACC	Reverse primer used in construction of pBB53odc1::gusA
02983gusF	GGATGCGGGTCAAGGTATC	Forward primer used in construction of pBB53odc2::gusA
02983gusR	TTGATGGTGTGCCATAGGA	Reverse primer used in construction of pBB53odc2::gusA
p53lw	ACAGGACGTAACATAAGGGAC T	Reverse primer for the <i>gusA</i> gene

856

857 **Supplementary Material Figure Legend**

858

859 **Fig. S1.** Analysis of PAs by mass spectrometry. As described in Methods, dansyl-
860 PAs were prepared from authentic standards or isolated from *S. meliloti* cells,
861 separated by HPTLC, eluted from the silica gel plates and characterized by matrix-
862 assisted laser desorption/ionisation (MALDI) high resolution, high mass accuracy
863 FT-ICR mass spectrometry (MS) and product ion tandem mass spectrometry
864 (MS/MS). The fragmentation diagrams and product ion spectra used in the
865 identification of the dansyl-PAs are presented in this figure. Panel (a), resolution
866 by HPTLC of dansyl-PA standards and unknown bound (spots B1 and B2) or free
867 (spots F1 through F3) PAs obtained from *S. meliloti* cells. Panel (b), structure of
868 the dansyl (DNS) chemical group. Panel (c), fragmentation diagram of DNS-Put.
869 Panel (d), product ion spectrum of DNS-Put standard. Standard Put (two amine
870 groups, so acquires two DNS groups; Fig. S1(c)) gave an intense signal for its
871 molecular species at m/z 555.20936 on MALDI FT-ICR mass spectrometry,
872 corresponding to an elemental composition $C_{28}H_{35}N_4O_4S_2$ ($M+H^+$ for (dansyl)₂Put;
873 0.1 ppm mass error) and a pattern of isotopic signals matching in relative
874 intensities very closely those predicted for this molecular composition. CID-MS-MS
875 of the ion at m/z 555 yielded a product ion spectrum consistent with (dansyl)₂Put
876 (Fig. S1(d)). The product ion at m/z 220 is related to that at m/z 234, by loss of one
877 O atom with transfer of two H atoms. Component F1 migrated similarly to standard
878 DNS-Put (Fig S1(a)). A strong signal was observed at m/z 555.20921 ($M+H^+$ for
879 (DNS)₂Put; 0.4 ppm mass error), and the product ion spectrum is (Fig. S1(e))
880 indistinguishable from that obtained from the authentic standard DNS-Put (Fig.
881 S1(d)), demonstrating that component F1 is Put. Panel (e), product ion spectrum
882 of spot F1 (see panel (a)), identified as DNS-Put. Panel (f), fragmentation diagram
883 of DNS-Spd. Panel (g), product ion spectrum of DNS-Spd standard. Standard Spd
884 (adds three dansyl groups; Fig. S1(f)) gave an intense $M+H^+$ signal at m/z
885 845.31810 ($C_{43}H_{53}N_6O_6S_3$; 0.2 ppm mass error), and a pattern of isotopic signals
886 that match very closely those predicted for a molecule with this composition. CID-
887 MS-MS of the ion at m/z 845 yielded a product ion spectrum consistent with

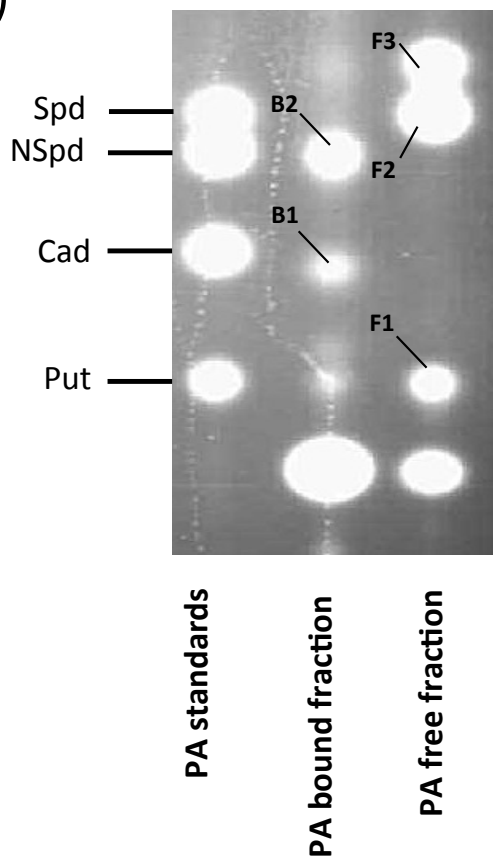
888 (dansyl)₃Spd (Fig. S1(g)). Component F2 migrated with the DNS-Spd standard
889 (Fig. S1(a)). A very strong signal was observed at m/z 845.31794 ($M+H^+$ for
890 (DNS)₃Spd; 0.5 ppm mass error), and the product ion spectrum (Fig. S1(h)) is very
891 similar to that from standard DNS-Spd (Fig. S1(g)), identifying the component as
892 DNS-Spd (Fig. S1(h)). Panel (h), product ion spectrum of spot F2 (see panel (a)),
893 identified as DNS-Spd. Panel (i), fragmentation diagram of DNS-NSpd. Panel (j),
894 product ion spectrum of DNS-NSpd standard. Standard NSpd (three dansyl
895 groups; Fig. S1(i)) gave an intense $M+H^+$ signal at m/z 831.30233 ($C_{42}H_{51}N_6O_6S_3$;
896 0.4 ppm mass error), and a pattern of isotopic signals that match very closely those
897 predicted for a molecule with this composition. CID-MS-MS of the ion at m/z 831
898 yielded a product ion spectrum consistent with (dansyl)₃NSpd (Fig. S1(j)). Panel
899 (k), product ion spectrum of spot B2 (see panel (a)), identified as DNS-NSpd.
900 Panel (l), fragmentation diagram of DNS-HSpd. Panel (m), product ion spectrum of
901 spot F3 (see panel (a)), identified as DNS-HSpd. Component B2 gave a signal at
902 m/z 831.30234 ($M+H^+$ for (DNS)₃NSpd; 0.4 ppm mass error) and a product ion
903 spectrum that identifies this component as NSpd (Fig. S1(k)). Component F3
904 migrated above DNS-Spd (Fig. S1(a)) and did not correspond with any of the PAs
905 for which authentic standards were available. Mass spectrometric analysis
906 generated a strong signal at m/z 859.33357 consistent with $M+H^+$ for
907 $C_{44}H_{55}N_6O_6S_3$, indicating a homologue of Spd with an additional CH_2 group (Fig.
908 S1(l); 0.4 ppm mass error). The product ion spectrum (Fig. S1(m)) is consistent
909 with (DNS₃)HSpd; note that the fragment ions at m/z 541 and 360 in the Spd
910 spectrum are shifted to m/z 555 and 374 in that of HSpd, consistent with the
911 presence of an additional backbone CH_2 group. The mass spectrum of a DNS-PA
912 that migrated similarly to a DNS-Cad standard on HPTLC plates (Fig. S1(a), spot
913 B1) gave an intense signal at m/z 569.22520 corresponding to an elemental
914 composition $C_{29}H_{37}N_4O_4S_2$ ($M+H^+$ for (DNS)₂diaminopentane; 0.2 ppm mass error)
915 and a pattern of isotopic signals matching in relative intensities very closely those
916 predicted for this molecular composition. The product ion spectrum was not
917 recorded, and so the substitution pattern was not determined. The identities of

918 DAP and NH₃ were assigned based only on their co-migration with DNS
919 derivatives of these compounds.

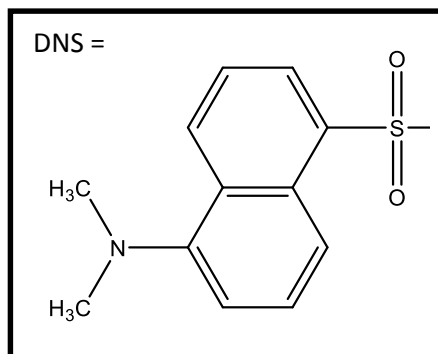
920

921

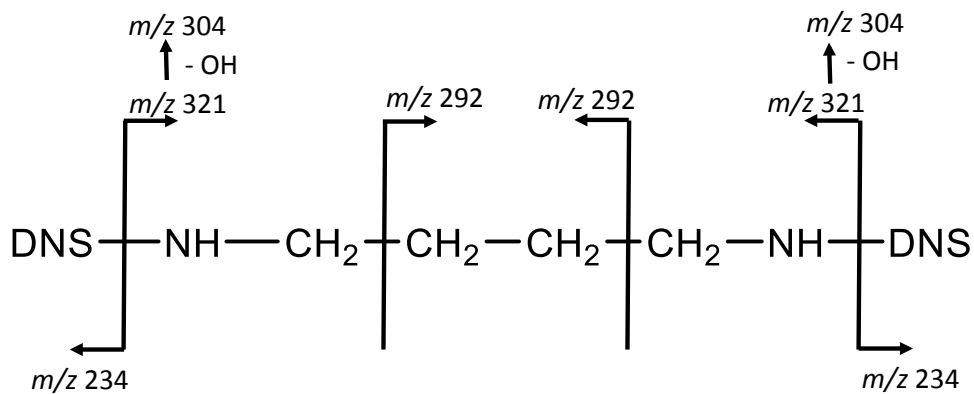
(a)



(b)

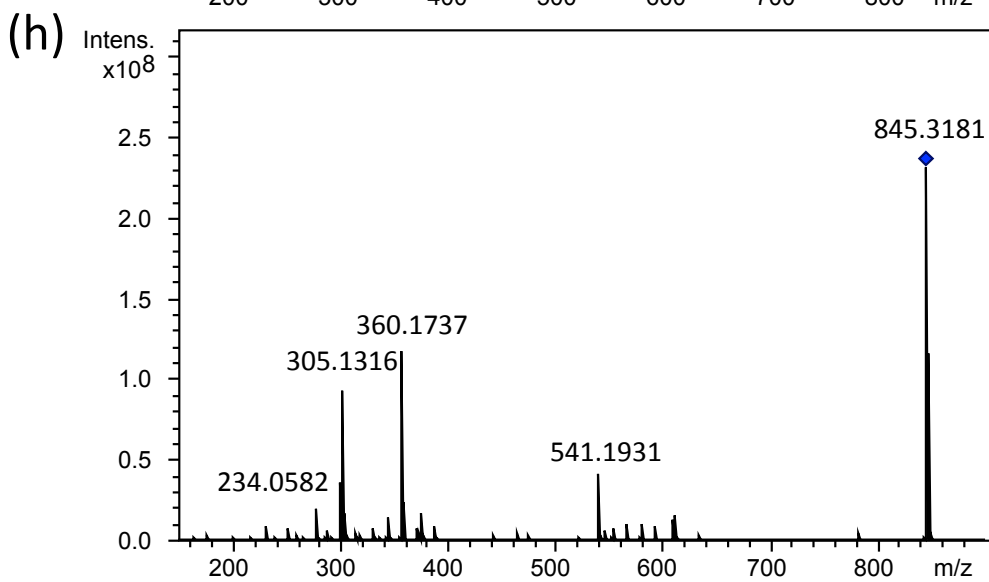
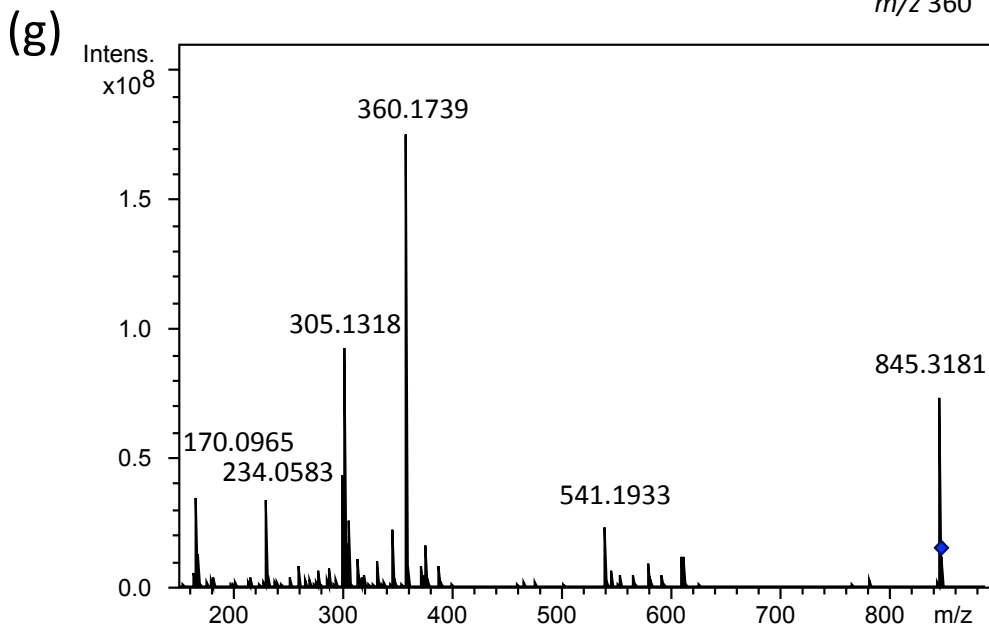
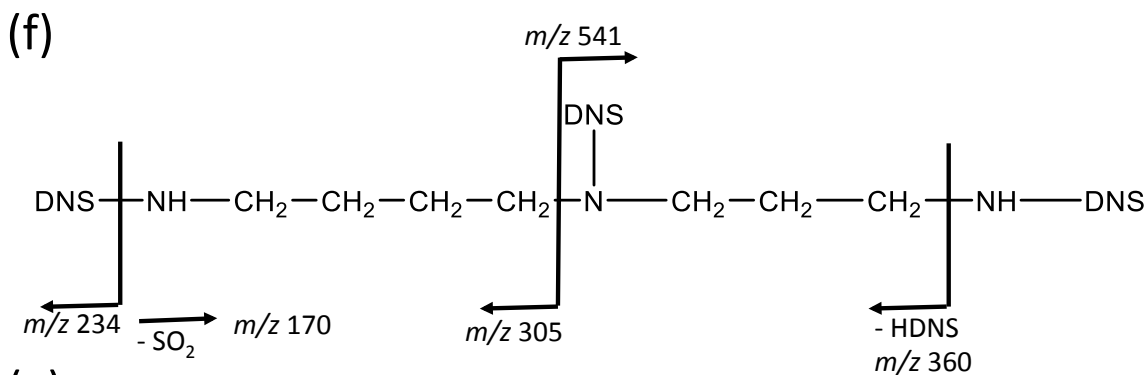


(c)



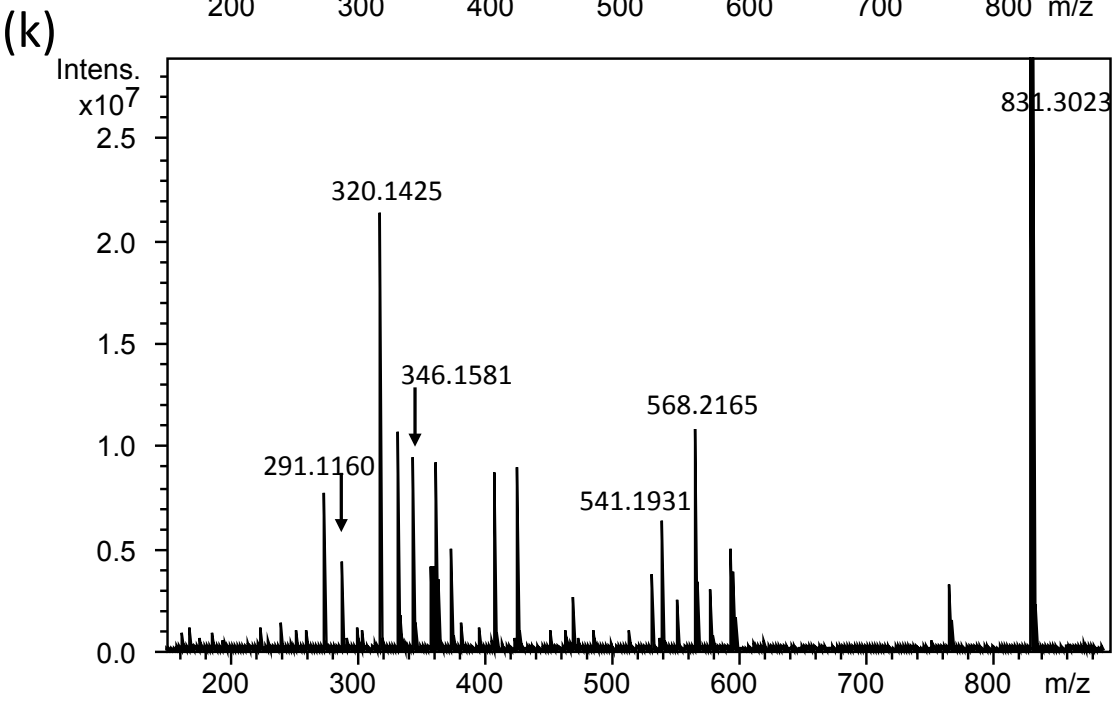
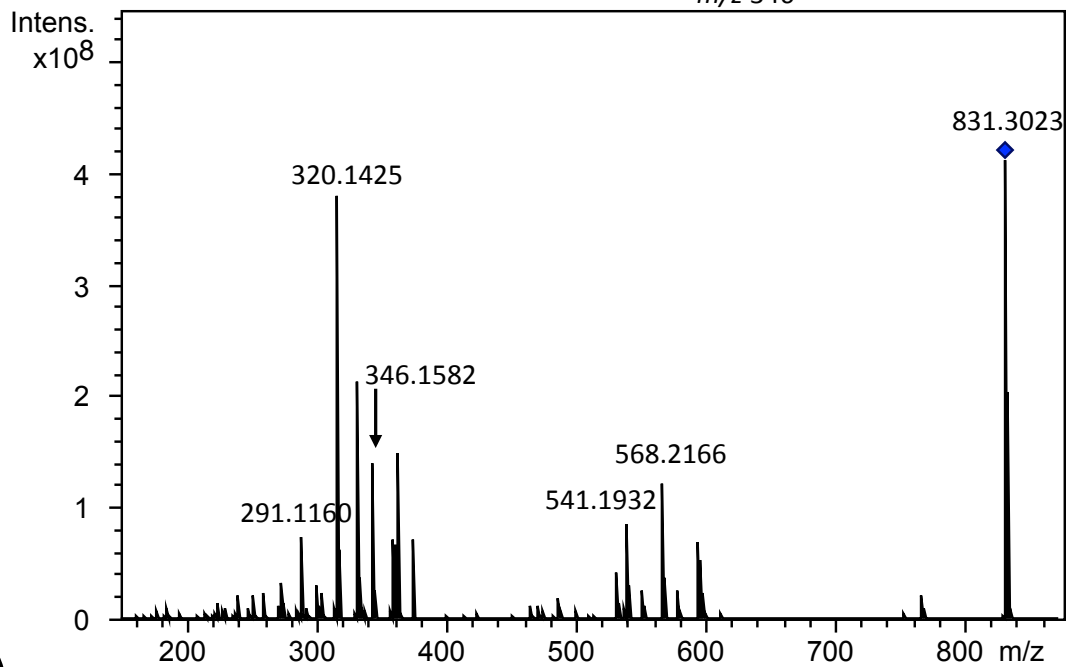
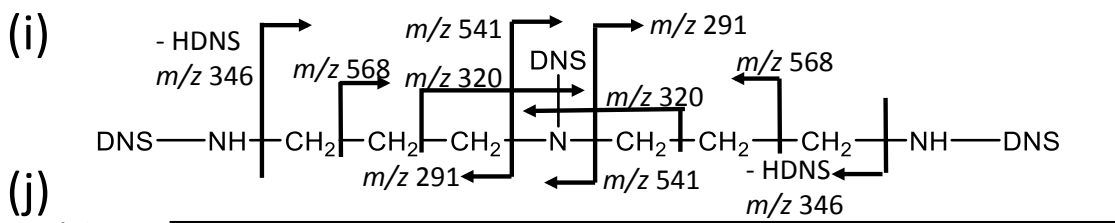
922

923



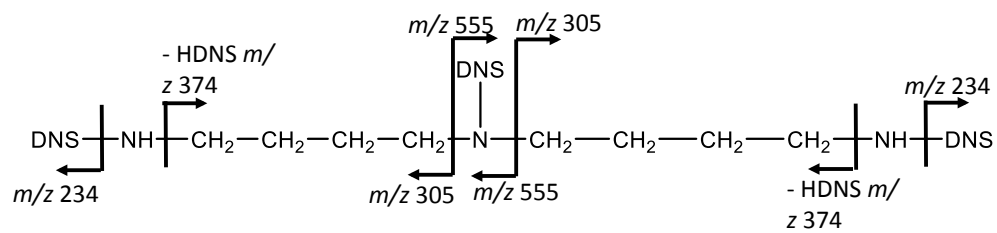
924

925

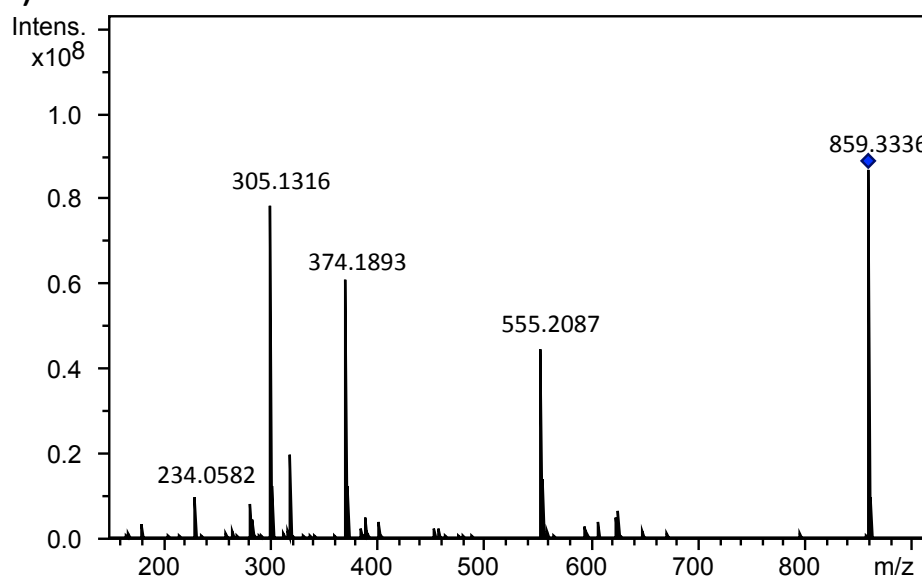


926
927

(l)



(m)



928

929 Fig. S1

930

931